Pergamon

Geochimica et Cosmochimica Acta, Vol. 67, No. 20, pp. 3859–3869, 2003

0016-7037/03 $30.00 + .00

doi:10.1016/S0016-7037(00)00309-0

Uptake of dissolved Cd by biogenic and abiogenic aragonite: a comparison with sorption onto calcite

MANUEL PRIETO,* PABLO CUBILLAS, and ÁNGELES FERNÁNDEZ-GONZALEZ
Departamento de Geología, Universidad de Oviedo, 33005 Oviedo, Spain

(*Received January* 7, 2003; revised 8 May 2003; *accepted in revised form May* 8, 2003)

Abstract—The uptake of Cd^{2+} by aragonite and calcite is investigated by combining macroscopic measurements with some qualitative sorption experiments performed in a hydrogel medium. Both biogenic and abiogenic aragonites were studied in order to evaluate the process on materials with different textures. Assuming that sorption occurs by surface precipitation of metal-bearing solids, the gel produces a drastic decrease in the nucleation density, which allows for the precipitation of crystallites that are large enough to be analysed by scanning electron microscopy and characterized by glancing-incidence X-ray techniques. The macroscopic study reveals that aragonite is a powerful sorbent for cadmium in aqueous environments. Microscopic observations indicate that cadmium is sorbed onto aragonite by surface precipitation of (Cd, Ca)CO_3 solid solutions with a calcite-type structure. The precipitating individuals grow randomly oriented on the surface to reach sizes in the micrometre range. As a consequence, the concentration of cadmium in the aqueous solution decreases dramatically to values controlled by the low solubility of the cadmium-rich end member. This mechanism involves simultaneous dissolution-crystallization and is the same for both abiogenic and biogenic aragonites, the only difference being a result of the higher specific surface area of the biogenic starting material. Long-term uptake of cadmium by calcite occurs through a similar dissolution-crystallization mechanism, the final outcome being virtually the same, that is, surface precipitation of (Cd,Ca)CO_3 solid solutions. In this case, however, substrate and precipitate are isostructural and the process occurs by oriented overgrowth of thin lamellar crystallites, which spread to quickly cover the surface by a layer a few nanometers thick. This epitaxial layer armors the substrate from further dissolution, so that the process stops when only a small amount of cadmium has been removed from the fluid. As a result, the "sorption capacity" of calcite is considerably lower than that of aragonite. The study illustrates reaction pathways and "partial" equilibrium endpoints in surface-precipitation processes involving solid solutions.

1. INTRODUCTION

Considerable experimental work on the interaction of cadmium and other divalent metals with the rhombohedral calcium carbonate, calcite, can be found in the geochemical literature. These studies embrace some related topics, including assessment of cadmium content in biogenic calcites (Boyle, 1981), measurements of distribution coefficients in coprecipitation reactions (e.g., Lorens, 1981; Königsberger et al., 1991; Reeder, 1996; Tesoriero and Pankow, 1996; Prieto et al., 1997; Fernández-González et al., 1999), and study of the sorption behaviour of this metal onto the surface of calcite crystals (McBride, 1980; Davis et al., 1987; Fuller and Davis, 1987; Zachara et al., 1991; Stipp et al., 1992; Chiarello et al., 1997). The subject is particularly important because calcite is a nearly ubiquitous mineral that can have a strong influence on the fate and transport of cadmium in soils, sediments and aquifers. While these studies have provided valuable information on the removal of cadmium and other toxic metals from solution by interaction with calcite, little is known about the sorption behaviour of cadmium onto the surface of aragonite, the second most important polymorph of $CaCO_3$. Due to its metastability under Earth's surface conditions, aragonite tends to transform into calcite by reaction with aqueous solutions, and a number of low-temperature experiments have focused on the effect of some ions on this solvent-mediated transformation (Bischoff and Fyfe, 1968; Berner, 1975; Böttcher, 1997). Other experimental work deal with the influence of divalent metals on the polymorphic precipitation of $CaCO_3$ in natural or industrial processes (Wada et al., 1995; Gutjahr et al., 1996), but studies of metal-sorption onto aragonite with respect to environmental problems are rare (Kornicker et al., 1985). Here, we examine the uptake of Cd^{2+} by aragonite and calcite in a comparative way. The study is carried out with both biogenic and abiogenic aragonites, to investigate the process on materials with different textures.

Sorption is, in the broad sense, the change of mass of a chemical in the solid phase as a result of mass-transfer between fluid and solid, which includes 1) true adsorption, 2) absorption or diffusion into the solid, and 3) surface precipitation to form an adherent phase that may consist of chemical species derived from both the aqueous solution and dissolution of the solid (Sposito, 1986). Sorption studies involve macroscopic and molecular level measurements that provide information at different scales about the products and the kinetics of these reactions (Brown et al., 1995). Macroscopic experiments are usually carried out by measuring the extent of uptake as a function of solution pH, concentration of sorbate in the aqueous solution, ionic strength, and time. Many investigators have studied the sorption rate of dissolved metals with calcite, invariably observing a rapid initial removal followed by a much slower uptake (McBride, 1979; McBride, 1980; Franklin and Morse, 1983; Fuller and Davis, 1987; Zachara et al., 1991). The fast

* Author to whom correspondence should be addressed (mprieto@geol.uniovi.es).

initial uptake is frequently interpreted as being the result of chemisorption, whereas the following slow removal is assumed to represent surface precipitation or coprecipitation.

In the case of cadmium, it is generally admitted from microscopic observations that long-term uptake by calcite occurs via surface precipitation of a Cd-bearing solid solution (Chiarello and Sturchio, 1994; Chiarello et al., 1997). In spite of this, macroscopic studies devoted to determine sorption isotherms rely primarily on a fast initial chemisorption stage, and are essentially focussed on this process. Most sorption experiments have been carried out with extremely low concentrations of cadmium and/or in the presence of complexing ligands (EDTA) to avoid saturation with respect to pure otavite ($CdCO_3$). However, as Tesoriero and Pankow (1996) have pointed out, if calcite is present, precipitation of Cd^{2+} as a carbonate solid solution will always occur, even when Cd^{2+} is present at trace levels, due to the strong tendency of this ion to partition into calcite. Therefore, this study is focussed on the surface-precipitation mechanism of removal of Cd^{2+} from solution, combining macroscopic measurements with microscopic observations. We are especially interested in comparing the sorption behaviour of calcite and aragonite in long-term "free-drift" sorption experiments, starting from a wide range of Cd^{2+} initial concentrations.

Macroscopic sorption measurements are usually carried out in stirred reactors where an aqueous solution containing the metal of interest is placed in contact with single-phase mineral powders. Such bulk methods monitor changes in the solution chemistry and provide some implicit information on the nature of the sorption process, but are insufficient to characterize the identity and stoichiometry of the sorbed entities. Macroscopic experiments need to be complemented by near-surface sensitive techniques capable of providing direct, molecular level information on the sorbate (Stipp et al., 1992; Chiarello et al., 1997). Even so, because the amount of material sorbed is small relative to the amount of sorbing solids, a full and unequivocal characterization of the sorption products (composition, growth mechanisms, spatial arrangement and crystallographic relations to the substrate, etc.) may be complicated. Here, we try to overcome these difficulties by improving the size of the "sorbed individuals," which is possible when sorption occurs by surface precipitation of a metal-bearing solid. With this aim, we have combined a macroscopic study with a number of qualitative sorption experiments achieved in a silica hydrogel medium. From experimental data, it is abundantly clear that hydrogels reduce the nucleation probability and increase the size of the precipitating crystals (Henisch, 1988; Lefaucheux and Robert, 1994; Prieto et al., 1994), which may facilitate the characterization of the sorbate (Prieto et al., 2002). In this way, we have determined the composition of the sorbate nuclei and their crystallographic relations to the substrate. We reacted Cd-bearing aqueous solutions with surfaces of calcite and aragonite crystals immersed in a gel so that sorption occurs by surface precipitation of Cd-bearing solids and the low nucleation density results in the precipitation of crystallites that are large enough to be observed and analyzed in a scanning electron microscope. The study is completed using glancing-incidence X-ray techniques to characterize the surface at different stages of the process.

2. EXPERIMENTAL METHODS

2.1. Macroscopic Measurements

Sorption experiments were carried out at 25 ± 0.1°C and at ambient partial pressure of CO_2 by reacting single-phase mineral solids with $CdCl_2$ aqueous solutions in a continuously stirred (100 rpm) thermostatic vessel. In all cases, 2 g of mineral grains, with diameters ranging from 1 mm up to 1.5 mm, were added to 100 cm^3 of reacting solution. Ambient CO_2 partial pressure was ensured by bubbling air (≈10 $cm^3 s^{-1}$) through the solution during the experiments. Three different kinds (A-aragonite, B-aragonite, and calcite) of solids were used. A-aragonite solids consist of aragonite grains that were obtained by crushing clear crystals of natural aragonite. Any fragments containing visual impurities (under magnification 100×) were removed and the remaining grains were ultrasonically cleaned in an ethanol bath and sieved to the selected size range. X-ray fluorescence analysis (Philips PW2404) of this starting material yielded ≈0.5 wt% foreign elements (Sr, Ba, Mg, Fe, Pb, Zn, Mn, Ni) but the presence of cadmium was undetected. These grains are roughly subhedral with some {110} cleavage surfaces exposed. B-aragonite consists of fragments of biogenic aragonite that were prepared in a similar way by crushing common cockle (*Cerastoderma edule*) shells. This material contains ≈0.7 wt% foreign elements (Mg, Sr, Na, Ba, Si, Al, Fe, Cu, Zn, Pb) but is free of cadmium. Although no other phases than aragonite were detected by X-ray diffraction, these cockleshell fragments could contain minor amounts of organic admixtures, small encrustations of detrital materials, inclusions, etc. In any case, the presence of these quantities of foreign elements is negligible in the context of the present study. Finally, calcite grains were obtained from optical-quality Iceland spar and are essentially cleavage fragments with only {1014} faces exposed. The specific BET surface areas of these starting materials were determined using an automatic volumetric gas adsorption apparatus (Micrometrics ASAP 2010) and N_2 (99.999% pure) at 77 K in the 10^{-6}-1 relative pressure range. They were 0.066 $m^2 \cdot g^{-1}$ for calcite, 0.29 $m^2 \cdot g^{-1}$ for A-aragonite, and 2.66 $m^2 \cdot g^{-1}$ for B-aragonite. The total pore volume was found to be negligible for A-aragonite (0.00059 $cm^3 \cdot g^{-1}$) and calcite (0.00021 $cm^3 \cdot g^{-1}$) but B-aragonite fragments were determined to be more porous (0.0102 $cm^3 \cdot g^{-1}$).

The initial aqueous solutions were prepared with reagent grade $CdCl_2$ (Merck) and deionized water (MilliQ system) at ambient CO_2 partial pressure. Concentrations of Cd^{2+} and Ca^{2+} in these initial aqueous solutions were more precisely determined by atomic absorption spectrophotometry (AAS, PYE-UNICAM SP90). The values shown in tables and figures for a reaction time $t = 0$ correspond to these analytical concentrations. In all cases, the parent solutions were virtually free of Ca^{2+}. Calculations using the geochemical code PHREEQC (Parkhurst, 1995) confirmed that these starting solutions were undersaturated with respect to otavite. For each starting solution (10, 5, 1, 0.5, and 0.1 mM), a set of experiments with increasing reaction times was carried out. The experiments were performed by placing 100 cm^3 (weighed to 0.001 g) of solution and 2.000 ± 0.005 g of mineral solids in the reacting vessel. After a given reaction period, the pH was measured and the solution was analysed for dissolved Cd^{2+} and Ca^{2+}. Concentration and pH evolution were monitored in this way for the first 3 d (0.5, 1, 1.5, 2, 2.5, 3, 4, 6, 10, 24, and 72 h). Moreover, some additional measurements were carried out after prolonged reaction times (7, 15, and 30 d).

The solution pH was measured with a combination electrode (Ross-Thermo-Orion 810200) and a digital pH-meter (CyberScan pH 2100, Eutech Ins.). Multipoint calibration of the electrode was performed with 4.01, 7.00, and 10.01 NIST-traceable buffers (Thermo-Orion). The solutions were analyzed for dissolved Ca^{2+} and Cd^{2+} by atomic absorption spectrophotometry (PYE-UNICAM SP90) in an air-acetylene flame following appropriate dilution. A set of standards, prepared from Ca^{2+} and Cd^{2+} AAS standard solutions (AccuStandard), was run before and periodically during each sampling event. Precision was determined to be ± 3% for Ca^{2+} and ± 2% for Cd^{2+}. When the concentration of Cd^{2+} decreased below the AAS detection-limit (<0.2 $\mu g \cdot g^{-1}$) the sample was analysed by inductively-coupled-plasma mass-spectrometry (ICP-MS, HP-4500) by using ^{115}In as internal standard, with a detection limit of ≈0.002 ng $\cdot g^{-1}$ and a precision of ± 1%. In the case of the experiments performed with calcite, the concen-

tration of calcium was also determined by ICP-MS by using ^{59}Co as internal standard, with a precision of ± 3%.

Each experimental run was conducted in triplicate, thus, the values reported in the figures are the average of three analogous experimental runs. The results are highly reproducible, particularly in the case of cadmium. The variation in Cd^{2+} concentration from replicate experiments at the same reaction time was always less than ± 4%. For calcium this variation was found to be within ± 5%.

2.2. Gel Experiments and Microscopic Observations

With the aim of improving the sorbate characterization, the macroscopic study was complemented with some "qualitative" sorption experiments performed in a silica hydrogel medium. One crystal of sorbent was placed at the bottom of a crystallizer that was then filled with 100 cm^3 of a sodium silicate (Na_2SiO_3) aqueous solution acidified with HCl 1M. After a few minutes, this solution polymerizes to form a gel that surrounds the crystal. Once a firm gel was formed, 100 cm^3 of a $CdCl_2$ aqueous solution were placed on the top of it without damaging its surface. This solution supplies Cd^{2+} ions and prevents the gel from drying. The silica hydrogel is a porous medium with a sheet-like structure that forms interconnecting cells (Henisch, 1988). The overall porosity and the water content depend on the concentration of the sodium silicate solution used and on the initial pH. For the Na_2SiO_3 solution used here (Merck, density 1.059 $g \cdot cm^{-3}$, pH 11.2), acidified with 1M HCl to a pH = 5.5, the "effective water" in the gel is ≈95.6 wt% and the pores have diameters from less than 0.1 μm up to 0.5 μm. This structure allows the gel to be used as a transport medium where convection and advection are suppressed, only allowing the diffusion of the aqueous ions, which can be sorbed on the surface of the immersed crystals. The experiments were performed using starting solutions with different concentrations (10 and 5 mM) of $CdCl_2$ (Merck, reagent grade). Calcite $\{10\bar{1}4\}$ and aragonite {110} crystal sections (≈25 mm^2 by 1 mm thick), with clean and smooth surfaces, were used as sorbent substrates. During the experiments the crystallizer was closed and its temperature was maintained at 25 ± 0.1°C.

For each type of substrate and parent solution, a set of experiments, with reaction times varying from 10 to 50 d, was carried out. After a set reaction period, the crystals were extracted from the gel to verify the incorporation of cadmium on their surfaces. For this purpose, the sorbent surfaces were examined in a scanning electron microscope (SEM, JEOL-6100) equipped with an energy-dispersive X-ray (EDX) spectrometer (Oxford-Instruments). Both secondary and backscattered electron images were obtained to determine the distribution of the sorbate onto the surfaces. Moreover, EDX microanalyses were carried out to detect the incorporation of cadmium onto the surface and occasionally to estimate sorbate compositions. SEM-observations were combined with a glancing incidence X-ray study (Philips-X'Pert-PRO) to improve the information obtained from the precipitate layer. Diffraction patterns were obtained by carrying out 2θ scans at a fixed small angle of incidence on the substrate surface.

3. RESULTS

3.1. Uptake of Dissolved Cadmium as a Function of Time

Figure 1 shows the decrease in Cd^{2+} concentration as a function of time for the sorption experiments performed with A-aragonite solids. As can be observed, there is a dramatic reduction of concentration in the early hours of the experiments. Starting from 0.1, 0.5, or 1 mM $CdCl_2$ aqueous solutions (Fig. 1a), the concentrations fall below the AAS detection-limit (0.2 $\mu g \cdot g^{-1}$ ≈0.0018 mM) in 10 h, and ICP-MS analyses yield Cd-concentrations in the nanomolar range for prolonged reaction times. The decrease is also dramatic in the experiments carried out with the more concentrated parent solutions, but in these cases the removal of dissolved cadmium is incomplete (Fig. 1b), which means that the uptake capacity of Cd^{2+} by the aragonite solids is not limitless. Although these time-concentration plots have a simple exponential appearance, the data

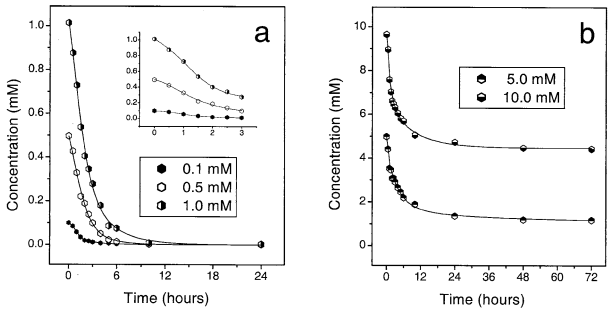

Fig. 1. Uptake of cadmium by abiogenic aragonite: evolution of Cd^{2+} concentration as a function of time. Note the different timescales in both graphs. (a) Parent solutions: 0.1, 0.5, and 1 mM $CdCl_2$. In the insert the curves are scaled up for short times. (b) Parent solutions: 5 and 10 mM $CdCl_2$.

points in Figure 1 do not fit well to single exponential-decay equations but to more complex S-shaped functions. This sigmoidal behaviour becomes apparent if one observes the graphs in the vicinity of $t = 0$ at a different scale (see insert in Fig. 1a), the uptake rate being moderate at the very beginning, then increasing to a maximum and finally decreasing to zero as the reaction goes to completion. Table 1 is a compilation of the initial analytical concentrations (C_0) of the parent solutions and the asymptotic concentration (C_∞) of cadmium after prolonged reaction times. For the experiments performed with a 5 mM parent solution (Fig. 1b) the concentration falls with time to an asymptotic value ≈0.99 mM, which corresponds to a Cd-uptake (U_∞) of 0.20 mmol per gram of aragonite (see Table 1), where

$$U_\infty = (C_0 - C_\infty)/20. \quad (1)$$

In this expression, the term $C_0 - C_\infty$ represents the number of millimoles of cadmium removed from one litre of solution, and the factor 20 is the weight of mineral solids per litre (i.e., 2 g in 100 cm^3) of solution.

Table 1. Uptake of cadmium (asymptotic values).

Parent solution $CdCl_2$ (mM)	C_0 (mM)	C_∞ (mM)	U_∞ (mmol $\cdot g^{-1}$)	U_∞/S_{BET} (mmol $\cdot m^{-2}$)
A-Aragonite				
10.0	9.65	4.39	0.26	0.91
5.0	4.98	0.99	0.20	0.71
1.0	1.01	<9.9E-5	—[a]	—
0.5	0.496	<6.3E-5	—[a]	—
0.1	0.099	<4.9E-5	—[a]	—
B-Aragonite				
10.0	9.65	3.80	0.30	0.11
5.0	4.98	0.56	0.22	0.083
1.0	1.01	<4.2E-5	—[a]	—
0.5	0.496	<3.5E-5	—[a]	—
0.1	0.099	<2.2E-5	—[a]	—
Calcite				
0.5	0.496	0.44	0.0028	0.040
0.1	0.099	0.078	0.0011	0.017

[a] For prolonged reaction times, there is a virtually complete Cd removal and considering a "limiting uptake capacity" has no meaning in these conditions (see Discussion).

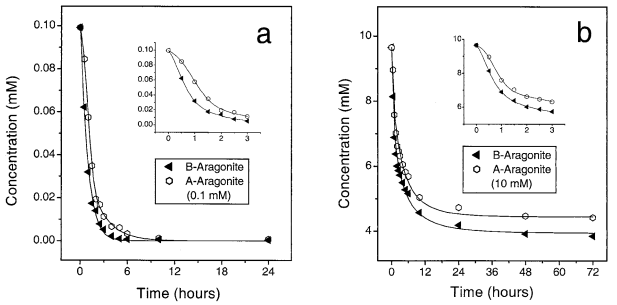

Fig. 2. Comparison between the uptake of cadmium by biogenic and abiogenic aragonite. The inserts show details for short reaction times. Note the different timescales in both plots. (a) Parent solution: 0.1 mM. $CdCl_2$. (b) Parent solution: 10 mM $CdCl_2$.

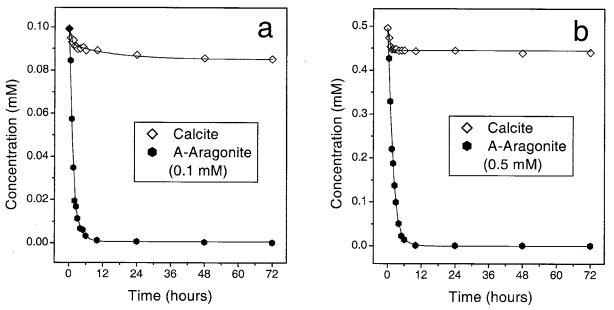

Fig. 3. Comparison between the uptake of cadmium by calcite and abiogenic aragonite. (a) Parent solution: 0.1 mM. $CdCl_2$. (b) Parent solution: 10 mM $CdCl_2$.

In the same way, starting from a 10 mM $CdCl_2$ solution, the concentration decreases to an asymptotic value (≈4.39 mM) that corresponds to the uptake of 0.26 mmol of cadmium per gram of aragonite. As we discuss later these "limiting amounts" do not correspond to equilibrium, but they are indicative of a situation where the reaction rate becomes virtually zero at a laboratory timescale. In contrast, in the experiments carried out using 0.1, 0.5, or 1 mM $CdCl_2$ solutions the concentration of cadmium in the fluid decreases to extremely low values, with U_∞ approaching $C_0/20$ mmol of cadmium per gram of aragonite, i.e., the removal of cadmium is "almost" complete when $t \rightarrow \infty$. The values of C_∞ compiled in Table 1 for these starting solutions correspond to 30 d of reaction but our measurements show that the concentrations continue to decrease for months at an extremely low rate.

The uptake of cadmium by biogenic aragonite follows a similar trend to that observed for A-aragonite. Figure 2 displays a comparison between both materials for the experiments carried out starting from 0.1 and 10 mM $CdCl_2$ aqueous solutions. As can be observed, the sorption of cadmium on B-aragonite is faster. Starting from a 0.1 mM $CdCl_2$ solution (Fig. 2a), the concentration falls below the AAS detection-limit reaching values in the nanomolar range after 10 h of reaction. The uptake by B-aragonite is also faster in the experiments carried out starting from 10 mM parent solutions (Fig. 2b), where the concentration falls towards an asymptotic limit (≈3.80 mM) that is below the value of C_∞ estimated for A-aragonite (Table 1). This limit corresponds to the uptake (U_∞) of 0.30 mmol of cadmium per gram of B-aragonite, that is, the amount of cadmium removed from the fluid is higher in the experiment carried out with biogenic aragonite. In the same way, starting from 5 mM $CdCl_2$ solutions the concentration decreases towards an asymptotic value ≈0.56 mM, which corresponds to the uptake of 0.22 mmol of cadmium per gram of B-aragonite.

It could be presumed that the higher uptake-rate by B-aragonite is due to its higher specific surface. However, attempts to establish a correlation between specific BET-areas (S_{BET}) and U_∞ do not support this. Although the specific BET-area of B-aragonite is almost 10 times larger than that of A-aragonite, the corresponding U_∞ values differ slightly and the ratios U_∞/S_{BET} for both B-aragonite and A-aragonite are significantly different (Table 1). As we will discuss later, this does not mean that the reactive-surface area is irrelevant for the sorption process. The question is if the BET-area is a good estimate of the reactive surface area in the present experiments, particularly for the biogenic material.

In contrast to sorption onto aragonite, the uptake of cadmium by calcite is much more limited. Figure 3 shows a comparison between the uptakes of cadmium by calcite and A-aragonite. Sorption onto calcite is considerably slower and tends to become negligible when the concentration of cadmium in the fluid is comparatively higher, i.e., the "sorption capacity" of calcite is very much less than that of A-aragonite. Although the specific BET-area of the calcite grains is smaller, the difference does not seem to be enough to explain such a different behaviour. The BET surface area-normalized uptake capacity (U_∞/S_{BET} in Table 1) of A-aragonite is almost two orders of magnitude larger than that of calcite. However, an analogous comparison between calcite and B-aragonite reveals that while the absolute uptake capacity of B-aragonite is two orders of magnitude higher than that of calcite (U_∞ values in Table 1), the uptake capacity normalized to the BET-area is not so different. This apparent inconsistency seems again to indicate that the BET-area is not a good estimate of the reactive surface area for the biogenic material.

3.2. Release of Calcium and pH Evolution

At the very beginning of the experiments the aqueous solution is virtually free of calcium, but the concentration increases as the $CaCO_3$ solids dissolve. Figure 4a shows the decrease of cadmium concentration and the simultaneous increase of dissolved calcium for the experiments carried out starting from 0.1 mM $CdCl_2$ solutions and A-aragonite solids. As can be observed, the concentration of calcium increases rapidly during the initial hours of the experiment. The relatively rapid dissolution is accompanied by an increase of the concentration of carbonate species in the aqueous solution, which leads to an increase of pH. This fast rise of pH occurs during the first hour (insert in Fig. 4a) and is then followed by a slow increase towards a limiting value. The release of calcium from B-aragonite follows a similar path, the only difference being a faster dissolution rate during the initial hours of the experiment that is also reflected by a faster increase of pH (Fig. 4b). In the experiments performed with calcite, however, the release of calcium is significantly slower and the concentration of this element after prolonged reaction times is low. Table 2 displays the limiting values ($t \rightarrow \infty$) for both pH and calcium concen-

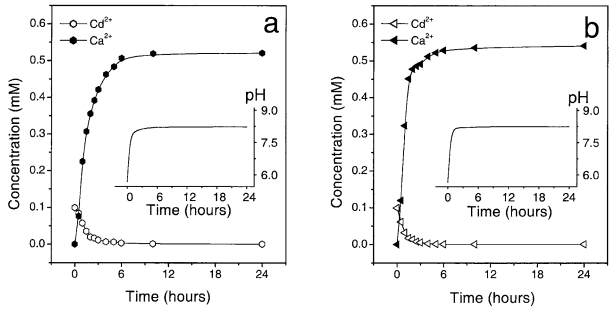

Fig. 4. Concentration of dissolved cadmium and calcium as a function of time. The inserts show the corresponding pH evolution. (a) Interaction of 0.1 mM $CdCl_2$ aqueous solutions with A-aragonite solids. (b) Interaction of 0.1 mM $CdCl_2$ aqueous solutions with calcite solids.

tration at various initial Cd^{2+} concentrations. Again, the upper limits are difficult to ascertain for the experiments carried out with aragonite and 1, 0.5, and 0.1 mM Cd^{2+} solutions because both removal and dissolution persist at very slow rates for months. The values compiled for these starting solutions correspond to 30 d of reaction.

It is worth noting that the final concentration of dissolved calcium (C_∞ in Table 2) virtually equals the amount of cadmium removed from the fluid ($C_0 - C_\infty$ in Table 2) in the experiments carried out with 10 and 5 mM parent solutions. This result obviously points towards a simple coupling between removal and dissolution (see section 4.2). In contrast, in the experiments performed with aragonite and less concentrated solutions (1, 0.5, and 0.1 mM) the removal of cadmium is almost complete ($C_0 - C_\infty \approx C_0$) and the final concentration of calcium does not show a clear relation with the amount of cadmium removed from the fluid. With calcite, however, the results indicate a simple coupling between removal and dissolution.

Table 2. Release of calcium and pH level after prolonged reaction times.

Parent solution $CdCl_2$ (mM)	C_∞ (calcium) (mM)	pH_∞	$C_0 - C_\infty$ (cadmium) (mM)
A-Aragonite			
10.0	5.27	6.26	5.26
5.0	4.08	6.54	3.99
1.0	0.58	8.26	1.01[a]
0.5	0.58	8.27	0.496[a]
0.1	0.60	8.28	0.099[a]
B-Aragonite			
10.0	5.96	6.30	5.85
5.0	4.44	6.61	4.41
1.0	0.601	8.28	1.01[a]
0.5	0.598	8.28	0.496[a]
0.1	0.611	8.29	0.099[a]
Calcite			
0.5	0.061	6.52	0.053
0.1	0.039	6.88	0.021

[a] For prolonged reaction times, there is a virtually complete removal of Cd so that $C_0 - C_\infty \approx C_0$ (see Table 1).

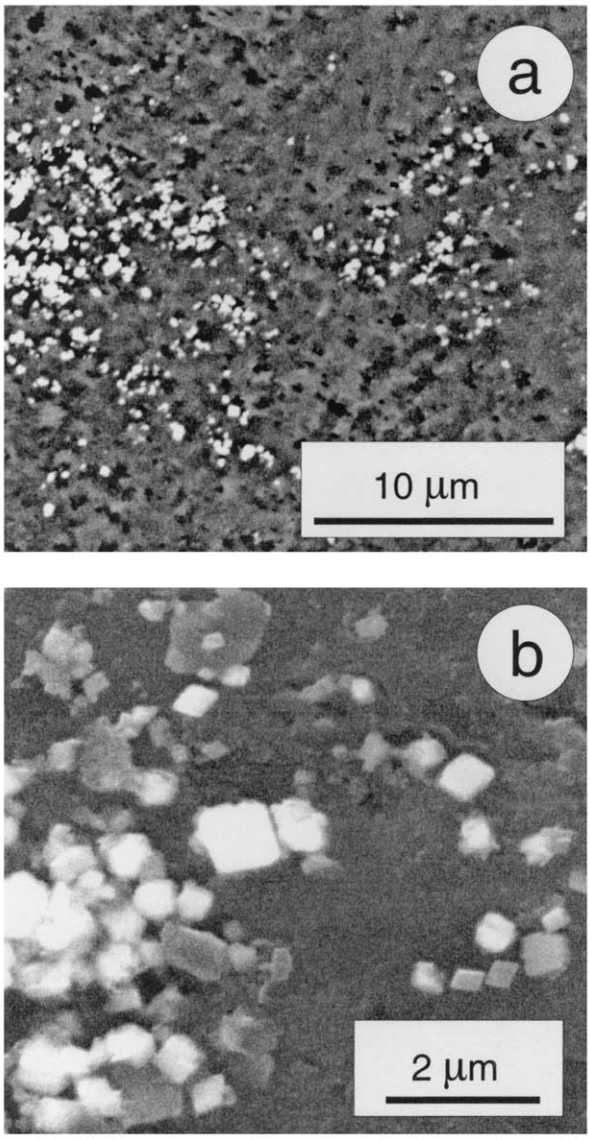

Fig. 5. Secondary electron image of an A-aragonite grain taken after 24 h of reaction with a 0.1 mM $CdCl_2$ aqueous solution. (a) General view. (b) Detail showing the rhombohedral appearance of the precipitating individuals.

3.3. Microscopic Observations

Figure 5a shows the surface of a typical A-aragonite grain after 24 h of reaction with a 0.1 mM $CdCl_2$ aqueous solution. The surface shows clear signs of dissolution and is covered by a precipitate consisting of numerous isolated individual crystals. Figure 5b is a higher magnification image showing individual crystallites of rhombohedral aspect with sizes ranging from 0.25 μm to 1 μm. The precipitate density increases with the Cd^{2+} concentration of the reacting solution, and the crystallites tend to concentrate in small aggregates. Finally, starting from 5 or 10 mM $CdCl_2$ solutions, the substrate becomes completely covered by a crust of precipitate during the first 24 h of reaction. Sorption of cadmium on B-aragonite occurs via formation of analogous precipitates, although a higher

nucleation density and a higher tendency to form aggregates was observed. In contrast, SEM-images of calcite grains, taken after a prolonged reaction with $CdCl_2$ aqueous solutions, do not show this kind of precipitate. Only in the vicinity of the cleavage macro-steps, where the $\{10\bar{1}4\}$ surface is damaged, small bright crystallites can be observed.

Sorption experiments carried out in a gel medium allow improvement of the previous observations: provided that sorption occurs by surface precipitation of Cd-bearing solids, the gel produces a drastic decrease in the nucleation density and this allows for the precipitation of individual crystals that are large enough to be analyzed in a scanning electron microscope. Figure 6a is the microphotograph of the {110} section of an aragonite crystal. The image was taken after 10 d of diffusion-reaction from a 5 mM $CdCl_2$ aqueous solution. As can be observed, the surface is covered by three-dimensional crystals with sizes ranging between 10 and 30 μm. These crystallites show the typical $\{10\bar{1}4\}$ rhombohedral morphologies of carbonates with a calcite-type structure. After a prolonged reaction time, the substrate becomes completely covered by rhombohedral crystals that form a crust on its surface (Fig. 6b). By monitoring the process at different stages, it is observed that the reaction does not proceed by growth onto a limited number of nuclei, where all of the nucleation occurred early in the experiments. In contrast, the process involves continuous nucleation and growth of new individuals until their mutual impingement. These overlaying crystals were confirmed to be members of the otavite-calcite series by X-ray diffraction. To avoid the inclusion of peaks from the substrate, the phase analysis was accomplished by carrying out a glancing incidence 2θ scan at a fixed angle (3°). The resulting diffraction pattern corresponds to a calcite type structure and is intermediate between calcite and otavite. The composition of the precipitating solid solution can be determined from the diffraction peak positions, given that the unit cell parameters vary linearly with composition between otavite and calcite (Borodin et al., 1979). In this particular case, both X-ray measurements and qualitative EDX microanalyses yield Cd-rich compositions of approximately $Cd_{0.975}Ca_{0.025}CO_3$. Starting from 10 mM $CdCl_2$ aqueous solutions the result is similar, although in this case the crystallites are richer in otavite, with mean compositions of about $Cd_{0.995}Ca_{0.005}CO_3$.

Gel experiments confirm that the long-term uptake of cadmium by calcite also occurs by surface precipitation of (Cd, Ca)CO_3 solid solutions. Figure 7a shows the backscattered electron image of the $(10\bar{1}4)$ surface of a calcite crystal after 10 d of reaction with a 5 mM $CdCl_2$ aqueous solution. Variations in composition lead to contrasts in image brightness, which allow numerous bright Cd-rich platelets to be visible. The platelets are delimited by polygonal contours parallel to the edges of the calcite substrate, which indicates a crystallographic orientation relationship between substrate and overgrowth. To illustrate this, traces of the $<\bar{4}41>$ calcite directions are superimposed on a region of the picture shown in Figure 7a. These crystallites were confirmed to be members of the otavite-calcite series by glancing incidence X-ray diffraction, using a 2θ scan recorded near the calcite $(10\bar{1}4)$ diffraction peak, at a fixed angle (2.5°) of incidence. As can be observed in Figure 7b, the substrate $(10\bar{1}4)$ diffraction peak is close to a smaller peak formed on the high 2θ side. One can interpret this peak as the $(10\bar{1}4)$ reflection of a Cd-rich otavite-calcite solid solution with a composition around $Cd_{0.97}Ca_{0.03}CO_3$. In agreement with previous observations (Chiarello et al., 1997), all

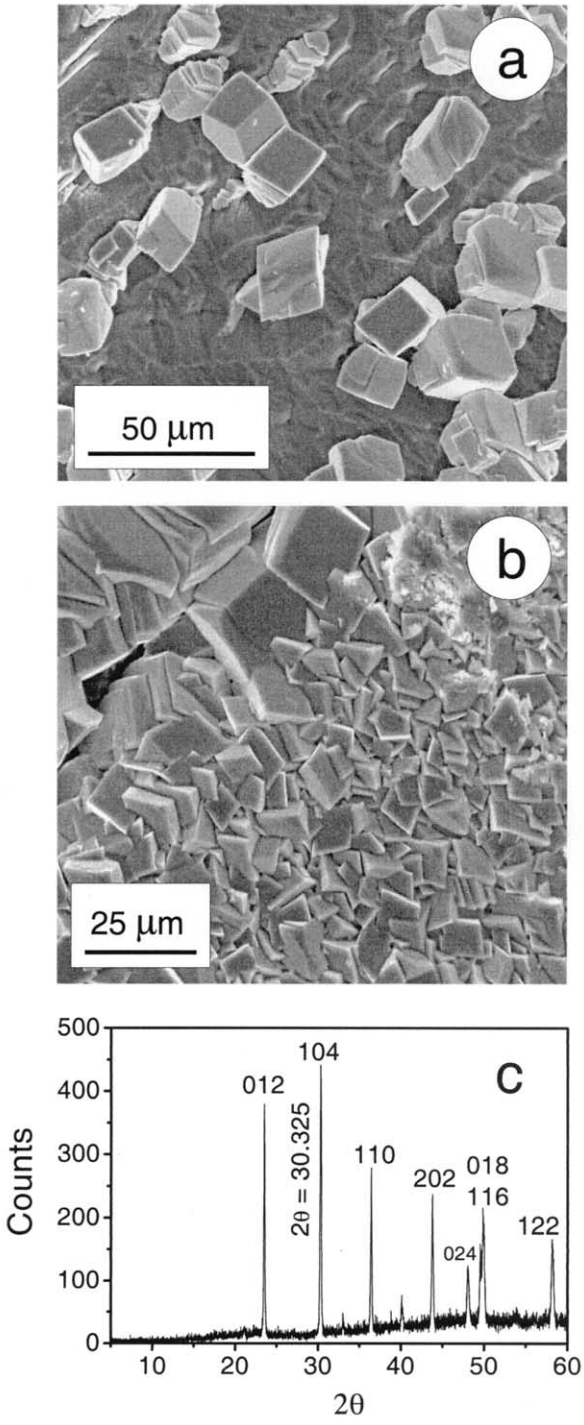

Fig. 6. Gel experiments. (a) Nucleation of (Cd, Ca)CO_3 crystallites on the {110}surface of an aragonite crystal (parent solution: 5 mM $CdCl_2$; diffusion time: 10 d). (b) Complete coating of the {110} surface of an aragonite substrate (Parent solution: 5 mM $CdCl_2$; diffusion time: 30 d). (c) X-ray diffraction 2θ scan recorded at a fixed angle (3°) of incidence.

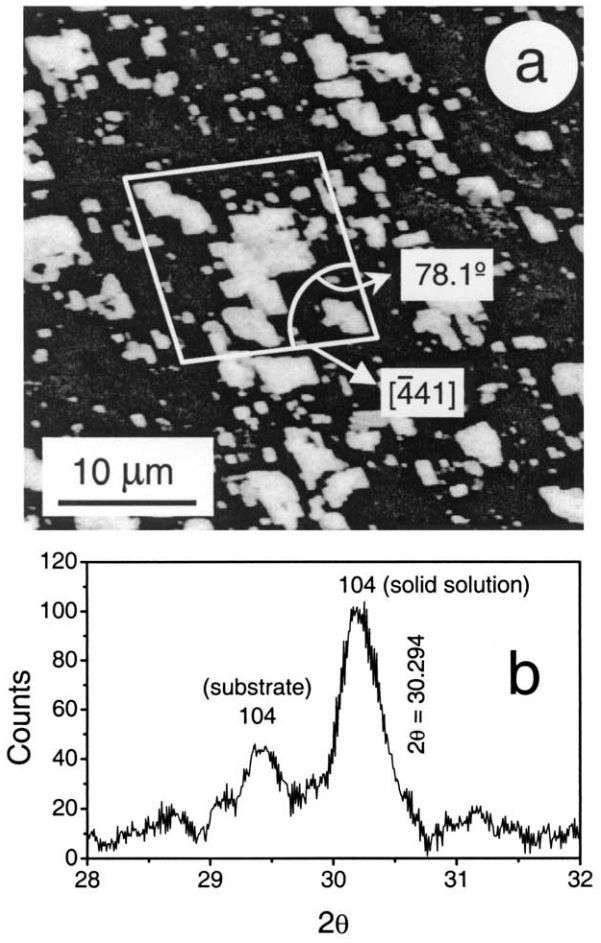

Fig. 7. Gel experiments. (a) Nucleation of (Cd, Ca)CO_3 platelets (BSE-image) on the {10$\bar{1}$4} surface of a calcite crystal (parent solution: 5 mM $CdCl_2$; diffusion time: 10 d). The traces represent the <$\bar{4}$41> directions corresponding to the calcite substrate. (b) X-ray diffraction 2θ scan recorded near the calcite (10$\bar{1}$4) diffraction peak at a fixed angle (2.5°) of incidence.

data indicate that the uptake of cadmium by calcite occurs via overgrowth of lamellar crystallites of a (Cd,Ca)CO_3 solid solution. Nucleation occurs in a nonrandom orientation with a strict parallelism between crystallographic directions of substrate and overgrowing crystals, as shown in Figure 7a. This is to be expected if one considers that calcite and cadmium carbonate (the ionic radii of Ca^{2+} and Cd^{2+} are 1.00 and 0.95 Å, respectively) form a solid solution where the lattice parameters vary slightly with the composition: heterogeneous nucleation is favored by close lattice match and close lattice match leads to oriented overgrowth or epitaxy. In this case, the lattice misfit along [$\bar{4}$41] is

$$f_{[\bar{4}41]} = ([\bar{4}41]_s - [\bar{4}41]_0)/[\bar{4}41]_s = 1.89\%, \quad (2)$$

where the subscripts "s" and "o" identify the [$\bar{4}$41] lattice translations corresponding to substrate and overgrowth, respectively. In spite of the important compositional difference, this misfit is small and one can expect a strong adhesion between substrate and overgrowth. As a consequence, the initial nuclei tend to spread as thin platelets, rather than to develop as thick three-dimensional crystallites (Chernov, 1984). In fact, the average crystallite size in the direction perpendicular to the substrate has been determined to be ≈200 Å by applying the Scherrer equation to the (10$\bar{1}$4) diffraction peak.

4. DISCUSSION

4.1. Interaction of Aragonite with 1, 0.5, and 0.1 mM $CdCl_2$ Aqueous Solutions

This work shows that the uptake of cadmium by aragonite occurs via surface precipitation of cadmium-rich (Cd,Ca)CO_3 solid solutions with a calcite-type structure. Such a mechanism involves the release of solutes (Ca^{2+} and CO_3^{2-} ions) from the mineral surface to the fluid and the reaction between the dissolved solute and the aqueous Cd^{2+} ions to form solid-solution nuclei. Thus, aragonite dissolution is concomitant with surface precipitation of (Cd,Ca)CO_3, resulting in a mechanism of sorption by coprecipitation. This sorption mechanism could be envisaged as a "solvent-mediated" transformation of aragonite to a calcite-type structure in the presence of Cd^{2+}, according to the reaction:

$$y \cdot Ca^{2+} + z \cdot Cd^{2+} + (CaCO_3)_{ar} \rightarrow (Cd_xCa_{(1-x)}CO_3)_{cal} + (y + x) \cdot Ca^{2+} + (z - x) \cdot Cd^{2+}, \quad (3)$$

which is analogous to the reaction proposed by Böttcher (1997) for the aragonite-calcite transformation under the influence of Mn^{2+} aqueous ions. In this reaction, the subscript x is related to y and z in a way that depends on the distribution coefficient of the substituting ions between fluid and solid. Here, the extremely low solubility of otavite compared to that of calcite results in a strong preferential partitioning of cadmium in the solid phase. Although there are some debates about the ideal or nonideal character of this solid solution (Davis et al., 1987; Königsberger et al., 1991; Stipp et al., 1992; Rock et al., 1994; Tesoriero and Pankow, 1996) most data seem to indicate that Cd^{2+} exhibits close to ideal behaviour when substituting for Ca^{2+} in calcite. Assuming an ideal solid solution, the equilibrium distribution coefficient for cadmium is given by the ratio of the solubility products (K_{otv} and K_{cal}) of the end members, namely

$$D_{Cd} = \frac{X_{Cd}}{X_{Ca}} \Big/ \frac{(Cd^{2+})}{(Ca^{2+})} = \frac{K_{cal}}{K_{otv}} = 4170, \quad (4)$$

where X_{Cd} and X_{Ca} are, respectively, the mole fractions of otavite and calcite in the solid, and the terms in parentheses represent the activities of the aqueous ions. Obviously, in addition to thermodynamics a number of kinetic/mechanistic effects can control ion partitioning during crystal growth (Lorens, 1981; Mucci and Morse, 1990; Paquette and Reeder, 1995). Nevertheless, according to the data compiled by Tesoriero and Pankow (1996), a value for D_{Cd} in the range of 1000−4500 is to be expected. This high value implies a strong tendency to form Cd-rich calcite precipitates, which accounts for the dramatic decrease of concentration of this ion observed in the fluid.

The driving forces operating during the process can be followed in Figure 8a, which displays the saturation index (SI) of the aqueous phase as a function of time for the experiments

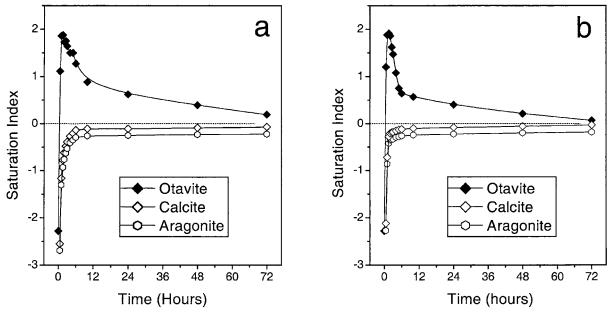

Fig. 8. Evolution of the saturation index of the experimental solution with respect to calcite, aragonite, and otavite, as a function of time. The data correspond to the interaction of 0.1 mM $CdCl_2$ aqueous solutions with (a) A-aragonite solids and (b) B-aragonite solids.

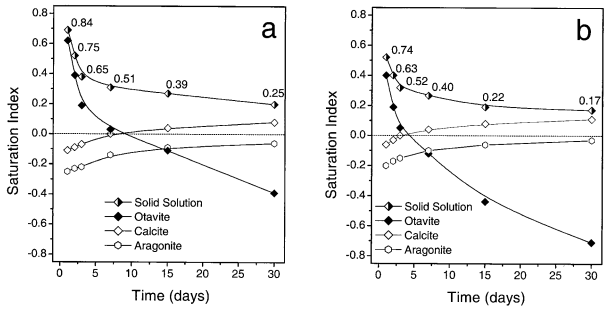

Fig. 9. Evolution of the saturation index with respect to calcite, aragonite, otavite, and (Cd, Ca)CO_3 solid solutions for prolonged reaction times. The labels indicate the composition of the solid-phase (i.e., X_{Cd}) for which the aqueous solution is most supersaturated. The solid-solution saturation indices correspond to these compositions. (a) Interaction of 0.1 mM $CdCl_2$ aqueous solutions with A-aragonite solids. (b) Interaction of 0.1 mM $CdCl_2$ aqueous solutions with B-aragonite solids.

performed with 0.1 mM $CdCl_2$ and A-aragonite. The saturation index was calculated by applying the geochemical code PHREEQC (Parkhurst, 1995) to the data shown in Figure 4a, which involves four calculation steps: 1) dissolution of $CdCl_2$ in water and equilibration with CO_2 at the atmospheric partial pressure, 2) dissolution of an amount of aragonite equivalent to the concentration of calcium released to the fluid, 3) precipitation of an amount of otavite equivalent to the quantity of cadmium removed from the fluid, and 4) equilibration of the resulting solution with CO_2 at the atmospheric partial pressure. The output of the calculation includes speciation of the aqueous solution, values of the saturation index with respect to the implied solid phases, alkalinity, and pH. This last value was fixed to the experimental pH to ensure consistency between analytical results and calculations.

At the very beginning of the experiment, the fluid is obviously undersaturated with respect to calcite, aragonite, and otavite, but the relatively fast dissolution of aragonite leads to a dramatic increase of the saturation index with respect to otavite, due to the low solubility of this mineral. The fluid becomes quickly supersaturated for this phase reaching a maximum ($SI_{otv} = 1.88$) during the first 1.5 h of the experiment. Afterwards, the continuous growth of Cd-rich solid solutions leads to a decrease of Cd^{2+} concentration in the fluid, and the saturation index gradually approaches zero. The saturation index with respect to calcite evolves differently, approaching zero from the undersaturation. Finally, because aragonite is more soluble than calcite, the saturation index with respect to aragonite remains lower. The evolution of the saturation index is fairly similar starting from 1.0 and 0.5 mM solutions, although the amount of precipitate is obviously different.

The uptake of cadmium by biogenic aragonite occurs by the same mechanism, the only difference being a consequence of the higher specific surface area of the starting material. Each shell fragment is a self-assembled crystalline aggregate that has more reactive surface than a similar single-crystal fragment, due to its finely crystalline, porous microstructure. The higher surface area yields a higher dissolution rate and, as a consequence, a higher saturation index in the early stages of the experiments (Fig. 8b). This in turn leads to a faster nucleation and growth of Cd-rich crystallites and, as a result, to a faster otavite "desupersaturation" pathway. In summary, the uptake of cadmium on biogenic aragonite occurs at a faster rate due to the higher surface area of the starting material. The fact that there is a disproportionate relationship between BET areas and sorption kinetics indicates, however, that the BET surface area is not a good estimate of the reactive surface area for dissolution/precipitation processes. Walter and Morse (1985) have demonstrated that only a fraction of the total BET surface area is actually available for dissolution. According to these authors, grain pores and fissures are isolated to varying degrees and may be filled with trapped solution that cannot exchange actively with the bulk solution. This effect is obviously more pronounced in the biogenic (more porous) grains, which tend to have substantially lower percentages of their total areas available for dissolution. As consequence, the BET surface area cannot be used as a reliable normalizing factor for comparison of biogenic/abiogenic dissolution rates. Moreover, in the present sorption experiments, there is a surface precipitation process that is also expected to be independent of the fine scale details involved in the BET determination.

It is worth noting that the otavite saturation index does not represent the actual supersaturation for the precipitating phase. In dealing with solid solutions, the supersaturation of a particular aqueous solution cannot be represented by a single value but by a function that depends on the solid-phase composition under consideration. This function has a "maximum" that corresponds to the composition of the solid solution for which that particular aqueous solution is most supersaturated (Prieto et al., 1993; Pina et al., 2000; Astilleros et al., 2003). For short reaction times, the precipitates are rich in cadmium and the otavite saturation index can be considered representative of the driving force, but, as the concentration of cadmium decreases, precipitation of solid solutions with an increasing calcium-content is to be expected. This is clear when considering the evolution of the supersaturation for prolonged reaction times. Figure 9 shows the evolution of the saturation index from 1 to 30 d of reaction. The calculations were performed for the same systems and by the same procedure as in Figure 8. As can be observed, the aqueous solution becomes undersaturated with respect to otavite during the first week of reaction. At this time, however, the system is supersaturated with respect to both the

calcite and calcite-otavite solid solutions, so that aragonite continues to dissolve and intermediate $(Cd,Ca)CO_3$ solid solutions grow. To illustrate this, Figures 9a and b also display the stoichiometric saturation indices with respect to the solid solutions for which the aqueous solutions are most supersaturated at each sampling time. The stoichiometric saturation indices (Glynn et al., 1990) were calculated assuming an ideal solid-solution behaviour, according to:

$$SI_{ss}(x) = log\left(\frac{[Cd^{2+}]^{x}[Ca^{2+}]^{(1-x)}[CO_3^{2-}]}{K_{otv}^{x}K_{cal}^{(1-x)}x^{x}(1-x)^{(1-x)}}\right), \qquad (5)$$

where $x = X_{Cd}$ and $1 - x = X_{Ca}$. At each time step, the composition of the solid solution that is most likely to precipitate corresponds to the one for which the aqueous solution is most supersaturated or has the "maximum" stoichiometric saturation index. Labels indicating these solid compositions (X_{Cd}) are shown near the corresponding data-points in Figures 9a and b. As can be observed, the value of X_{Cd} for which the fluid is most supersaturated decreases with the reaction time, so that a compositional evolution of the precipitate is to be expected. It is worth noting here that most of the cadmium is removed from the fluid during the first 10 h of the experiment (not shown in Fig. 9), that is, when the maximum supersaturation corresponds to Cd-rich ($X_{Cd} > 0.95$) solid solutions. As a consequence, the initial Cd-rich crystallites could ultimately become surrounded by a calcium-rich layer, resulting in the main mass of pollutant being isolated from the fluid. In fact, sharp compositional zoning from a cadmium-rich core to a calcium-rich rim has been observed in crystallizing single-crystals of this solid solution (Prieto et al., 1997; Fernández-González et al., 1999), and a similar zoning could occur in these experiments.

Obviously, after 30 d the reactions are not complete and the concentration of cadmium in the fluid continues to decrease for months towards extremely low values. The end point to which the system tends is, however, difficult to estimate. True thermodynamic equilibrium would require complete dissolution-recrystallization to form a unique and homogeneous (Cd, Ca)CO_3 solid phase, whose composition is easy to calculate by solving a set of equilibrium, charge balance, and mass balance equations (Lippmann, 1980; Glynn et al., 1990). Starting with 100 cm^3 of a 0.1 mM $CdCl_2$ aqueous solution and 2 g of aragonite solids this end point would imply equilibrium between a homogeneous Cd-poor solid (X_{Cd} = 4.98E-4) and an extremely Cd-poor (7.00E-8 mM) aqueous solution. This state is rather unrealistic and although all the aragonite solids dissolve and recrystallize as $(Cd,Ca)CO_3$ solid solutions, the newly formed crystals would be zoned with only the outer layer remaining at equilibrium with the fluid.

Finally, although during the first hours of the process the otavite saturation index attains values around 1.8, this supersaturation does not seem to be enough for spontaneous, homogeneous nucleation. In fact, it is abundantly accepted in the crystal growth literature that spontaneous nucleation of sparingly soluble substances with high interfacial tension requires significant degrees of supersaturation (Berner, 1971; Mullin, 1993; Sarig, 1994). In general terms, the lower the solubility of a crystal in a solvent, the larger is the supersaturation needed for spontaneous, homogeneous nucleation. In the case of calcite, a saturation index $\approx$ 2.60 was reported as the limit between heterogeneous and homogeneous nucleation, in experiments carried out by mixing $CaCl_2$ and Na_2CO_3 aqueous solutions (Mullin, 1993). Since otavite is considerably less soluble than calcite, higher values of the saturation index should be needed for the spontaneous, homogeneous nucleation of calcite-otavite solid solutions. This explains that all of the $(Cd,Ca)CO_3$ nucleation that occurred in the sorption experiments took place on aragonite surfaces. Our finding is consistent with the observations by Berndt and Seyfried (1999), who found newly formed, fine grained calcite attached to the surfaces of aragonite grains in their study of the conversion of aragonite to calcite in pollutant-free aqueous solutions.

Table 3. Interaction of aragonite with 5 and 10 mM $CdCl_2$: saturation indices after prolonged reaction times.

Parent solution $CdCl_2$ (mM)	SI_{cal}	SI_{arag}	SI_{otv}	X_{Cd}[a]
A-Aragonite				
10.0	−3.18	−3.32	0.06	0.999
5.0	−2.72	−2.86	0.08	0.998
B-Aragonite				
10.0	−3.07	−3.21	0.04	0.999
5.0	−2.52	−2.66	−0.01	0.997

[a] Solid-phase composition for which the fluid is most supersaturated.

4.2. Interaction of Aragonite with 5 and 10 mM $CdCl_2$ Aqueous Solutions

When the initial concentration of the reacting solution is higher, the precipitate can armour the substrate from further dissolution, so that the process stops, at least at a laboratory timescale. This is clear in the experiments using 5 and 10 mM $CdCl_2$ aqueous solutions, in which the process is virtually interrupted (Fig. 1b and Table 1) when the concentration of cadmium in the fluid (0.99 and 4.39 mM, respectively) is quite high. The effect can be explained by the development of a crust of precipitate (similar to that shown in Fig. 6b) that completely covers the aragonite grains. Obviously, at this stage the system is not at equilibrium (equilibrium implies the development of an unique solid-phase with an homogenous composition satisfying Eqn. 4) but the term "partial equilibrium" (Helgeson, 1968) could be used to describe a situation where the initial reacting solid becomes isolated from the aqueous solution by a coating of secondary solids. This becomes evident by calculating the saturation indices of the aqueous solutions for $t \rightarrow \infty$. The results, shown in Table 3, were obtained from the data compiled in Tables 1 and 2 by applying the method described in section 4.1. Given the unavoidable inaccuracy of the chemical analyses, one can consider the aqueous solution to be at saturation for nearly pure otavite ($X_{Cd} > 0.99$), and undersaturated for all other solid phases (Table 3). Obviously, this outcome can only be explained by the presence of a layer of nearly pure otavite, at equilibrium with the aqueous solution, which covers completely the substrate. Further, the fact that the composition of this layer is nearly pure otavite accounts for the results shown in Table 2 and section 3.2, where the concentration of calcium released to the fluid was found to be equivalent to the concentration of cadmium removed from it.

Table 4. Interaction of calcite with 0.5 and 0.1 mM $CdCl_2$: saturation indices after prolonged reaction times.

Parent solution $CdCl_2$ (mM)	SI_{cal}	SI_{arag}	SI_{otv}	X_{Cd}[a]
0.5	−4.42	−4.56	0.03	0.999
0.1	−3.87	−4.01	0.04	0.997

[a] Solid-phase composition for which the fluid is most supersaturated.

4.3. Uptake of Cadmium by Calcite

The uptake of cadmium by calcite occurs through a dissolution-recrystallization mechanism that is similar to that described by Eqn. 3, to be exact

$$y \cdot Ca^{2+} + z \cdot Cd^{2+} + (CaCO_3)_{cal} \rightarrow (Cd_xCa_{(1-x)}CO_3)_{cal} + (y + x) \cdot Ca^{2+} + (z - x) \cdot Cd^{2+}. \quad (6)$$

Obviously, in this case the process only implies changes in chemistry, the solid phases involved being both calcite-type. The overall reaction requires dissolution of calcite instead of aragonite, which accounts for the smaller sorption rate observed in these experiments: calcite is less soluble than aragonite and, as a consequence, the dissolution rate of calcite is slower. This fact, however, does not explain the considerably lower sorption-capacity of the calcite solids (Fig. 3). Starting from either calcite or aragonite the final product is virtually the same, a solid solution very rich in cadmium. However, the final values of dissolved cadmium are very different.

An explanation of this apparent incongruity needs to consider not only the chemistry of the sorbate but also its crystallographic relationships with the sorbent. On calcite, the uptake of cadmium entails epitaxial nucleation of thin lamellar crystallites, which spread to quickly cover the surface by a layer of nanometric thickness. This epitaxial layer armors the substrate from further dissolution, so that the system reaches a state of "partial" equilibrium when only a small amount of cadmium has been removed from the fluid (Table 4). In contrast, the uptake of cadmium by aragonite occurs by heterogeneous nucleation of three-dimensional crystallites distributed in a random orientation on a surface with a different structure. These crystallites develop isometrically to reach sizes in the micrometric range. Clearly, the mass of precipitate needed to cover the aragonite grains is drastically larger than the mass required to envelop an identical amount of calcite by an epitaxial layer, which explains the higher sorption capacity of the aragonite solids.

5. CONCLUSIONS

The present experiments demonstrate that cadmium interacts strongly with aragonite in aqueous environments. Microscopic observations indicate that cadmium incorporates onto aragonite by surface precipitation of $(Cd,Ca)CO_3$ solid solutions with a calcite-type structure. As a consequence, the concentration of cadmium in the aqueous solution decays dramatically to reach values controlled by the extremely low solubility of the otavite end member. The process is obviously associated to simultaneous dissolution-recrystallisation and could be envisaged as a solvent-mediated transformation of aragonite to a calcite-type structure with the corresponding changes in chemistry. The mechanism is similar for both abiogenic and biogenic aragonites, the only difference being a consequence of the higher specific surface of the biogenic starting material.

In summary, aragonite appears to be a powerful sorbent for cadmium in aqueous environments. Shell fragments are particularly reactive due to the micrometric scale of the constituting individual crystals. Although the "sorption capacity" is limited by the amount of precipitate that can be formed without armoring the substrate surface from further dissolution, this limit is high because it involves the development of a "crust" of micrometric thickness. The results contrast with the limited sorption capacity displayed by calcite fragments of similar size. The uptake of cadmium by calcite occurs through a similar dissolution-crystallization mechanism, the final outcome being virtually the same, i.e., surface precipitation of $(Cd,Ca)CO_3$ solid solutions. However, in this case the substrate and precipitate are isostructural and the process occurs by oriented overgrowth of thin lamellar crystallites, which spread to quickly cover the surface by a layer of nanometric thickness. This epitaxial layer armors the substrate from further dissolution, so that the process stops when only a small amount of cadmium has been removed from the fluid.

From a kinetic point of view, the overall rate of a solvent-mediated transformation depends on both the growth rate of the stable phase and the dissolution rate of the metastable phase. Cardew and Davey (1985) propose a model to explore polymorphic transformations in the presence of seeds of the stable polymorph. According to these authors, the "desupersaturation" profile that is observed during the transformation depends strongly on the relative kinetics of growth and dissolution, so that the shape of this profile can be used to fit kinetic parameters. Obviously, a model developed for isochemical transformations cannot be applied directly to a process where the newly formed crystals have not only a different structure but also a variable composition. On the other hand, the fact that the precipitate progressively covers the substrate surface affects the reaction kinetics, since the area that is available for dissolution decreases during the process. Nicholson et al. (1990) use a kinetic model that combines the surface reaction with the accumulation of a product layer to fit their experimental data for pyrite oxidation. This model, referred to as the "shrinking-core" model (Wen, 1968), has demonstrated to be an excellent predictor of the rate of oxidation over time and could be incorporated into a kinetic model for the experiments described in the previous sections. Kinetic modelling is, however, beyond the scope of the present work, which is essentially focussed on both the mechanisms and the reaction pathways of the sorption process. Future papers will deal with this matter.

Acknowledgments—This work was supported by the European Commission (contract HPRN-CT-2000-058) and by the Ministry of Science and Technology of Spain (grant BTE2000-0300). We thank David Heasman for his insightful comments. Electron microscopy, X-ray diffraction, and ICP-MS analyses were carried out by Central Scientific Services of the University of Oviedo. We thank Manuel Díez Tascón for the BET measurements. The helpful comments of A. Mucci and three anonymous reviewers substantially improved the manuscript.

Associate editor: A. Mucci

REFERENCES

Astilleros J. M., Pina C. M., Fernández-Díaz L., and Putnis A. (2003) Supersaturation functions in binary solid-solution-aqueous solution systems. *Geochim. Cosmochim. Acta* **67**, 1601–1608.

Berner R. A. (1971) *Principles of Chemical Sedimentology.* McGraw-Hill.

Berner R. A. (1975) The role of magnesium in the crystal growth of calcite and aragonite in seawater. *Geochim. Cosmochim. Acta* **39**, 489–504.

Bischoff J. L. and Fyfe W. S. (1968) Catalysis, inhibition, and the calcite-aragonite transformation. *Am. J. Sci.* **266**, 65–79.

Borodin V. L., Lyutin V. I., Ilyukhin V. V., and Belov N. V. (1979) Isomorphous calcite-otavite series. *Sov. Phys. Dokl.* **24**, 226–227.

Böttcher M. (1997) The transformation of aragonite to $Mn_xCa_{(1-x)}CO_3$ solid-solutions at 20°C: An experimental study. *Mar. Chem.* **57**, 97–106.

Boyle E. A. (1981) Cadmium, zinc, copper, and barium in foraminifera tests. *Earth Planet. Sci. Lett.* **53**, 11–35.

Berndt M. E. and Seyfried W. E. (1999) Rates of aragonite conversion to calcite in dilute aqueous fluids at 50 to 100°C: Experimental calibration using Ca-isotope attenuation. *Geochim. Cosmochim. Acta* **63**, 373–381.

Brown G. E., Parks G. A., and O'Day P. A. (1995) Sorption at mineral-water interfaces: Macroscopic and microscopic perspectives. In *Mineral Surfaces* (eds. D. J. Vaughan and R. A. D. Pattrick), pp. 129–183. Chapman and Hall.

Cardew P. T. and Davey R. J. (1985) The kinetics of solvent-mediated phase transformations. *Proc. R. Soc. Lond. A* **398**, 415–428.

Chernov A. A. (1984) *Modern Crystallography III: Crystal Growth.* Springer-Verlag.

Chiarello R. P. and Sturchio N. C. (1994) Epitaxial growth of otavite on calcite observed in situ by synchrotron X-ray scattering. *Geochim. Cosmochim. Acta* **58**, 5633–5638.

Chiarello R. P., Sturchio N. C., Grace J. D., Geissbuhler P., Sorensen L. B., Cheng L., and Xu S. (1997) Otavite-calcite solid-solution formation at the calcite-water interface studied in situ by synchrotron X-ray scattering. *Geochim. Cosmochim. Acta* **61**, 1467–1474.

Davis J. A., Fuller C. C., and Cook A. D. (1987) Mechanisms of trace metal sorption by calcite: Adsorption of Cd^{2+} and subsequent solid solution formation. *Geochim. Cosmochim. Acta* **51**, 1477–1490.

Fernández-González A., Prieto M., Putnis A., and López Andrés S. (1999) Concentric zoning patterns in crystallizing $(Cd,Ca)CO_3$ solid solutions from aqueous solutions. *Min. Mag.* **63**, 331–343.

Franklin M. L. and Morse J. W. (1983) The interaction of manganese(II) with the surface of calcite in dilute solutions and seawater. *Mar. Chem.* **12**, 241–254.

Fuller C. C. and Davis J. A. (1987) Processes and kinetics of Cd^{2+} sorption by a calcareous aquifer sand. *Geochim. Cosmochim. Acta* **51**, 1491–1502.

Glynn P. D., Reardon E. J., Plummer L. N., and Busenberg E. (1990) Reaction paths and equilibrium end-points in solid-solution aqueous-solution systems. *Geochim. Cosmochim. Acta* **54**, 267–282.

Gutjahr A., Dabringhaus H., and Lacmann R. (1996) Studies of the growth and dissolution kinetics of the $CaCO_3$ polymorphs calcite and aragonite II. The influence of divalent cation additives on the growth and dissolution rates. *J. Cryst. Growth* **158**, 310–315.

Helgeson H. C. (1968) Evaluation of irreversible reactions in geochemical processes involving minerals and aqueous solutions—I. Thermodynamic relations. *Geochim. Cosmochim. Acta* **32**, 853–877.

Henisch H. K. (1988) *Crystals in Gels and Liesegang Rings.* Cambridge University Press.

Königsberger E., Hausner R., and Gamsjäger H. (1991) Solid-solute phase equilibria in aqueous solution. V: The system $CdCO_3$-$CaCO_3$-CO_2-H_2O. *Geochim. Cosmochim. Acta* **55**, 3505–3514.

Kornicker W. A., Morse J. W., and Damasceno R. (1985) The chemistry of Co^{2+} interaction with calcite and aragonite surfaces. *Chem. Geol.* **53**, 229–236.

Lefaucheux F. and Robert M. C. (1994) Crystal growth in gels. In *Handbook of Crystal Growth 2* (ed. D. T. J. Hurle), pp. 1271–1303. Elsevier.

Lippmann F. (1980) Phase diagrams depicting the aqueous solubility of binary mineral systems. *N. Jb. Miner. Abh.* **139**, 1–25.

Lorens R. B. (1981) Sr, Cd, Mn, and Co distribution coefficients in calcite as a function of calcite precipitation rate. *Geochim. Cosmochim. Acta* **45**, 553–561.

McBride M. B. (1979) Chemisorption and precipitation of Mn^{2+} at $CaCO_3$ surfaces. *J. Soil Sci. Am.* **43**, 693–698.

McBride M. B. (1980) Chemisorption of Cd^{2+} on calcite surfaces. *J. Soil Sci. Am.* **44**, 26–28.

Mucci A. and Morse J. W. (1990) Chemistry of low-temperature abiotic calcites: Experimental studies on coprecipitation, stability and fractionation. *Aquatic Sci.* **3**, 217–254.

Mullin J. W. (1993) *Crystallization*. 3rd ed. Butterworth-Heinemann.

Nicholson R. V., Gillham R. W., and Reardon E. J. (1990) Pyrite oxidation in carbonate-buffered solution: 2. Rate control by oxide coatings. *Geochim. Cosmochim. Acta* **54**, 395–402.

Paquette J. and Reeder R. J. (1995) Relationship between surface structure, growth mechanism, and trace element incorporation in calcite. *Geochim. Cosmochim. Acta* **59**, 735–749.

Parkhurst D. L. (1995) *User's Guide to PHREEQC—A Computer Program for Speciation, Reaction Path, Advective-Transport, and Inverse Geochemical Calculations.* Water-Resources Investigations Report 143. U.S. Geological Survey.

Pina C. M., Enders M., and Putnis A. (2000) The composition of solid solutions crystallising from aqueous solutions: The influence of supersaturation and growth mechanisms. *Chem. Geol.* **168**, 195–210.

Prieto M., Putnis A., and Fernández-Díaz L. (1993) Crystallization of solid solutions from aqueous solutions in a porous medium: Zoning in $(Ba,Sr)SO_4$. *Geol. Mag.* **130**, 289–299.

Prieto M., Putnis A., Fernández-Díaz L., and López-Andrés S. (1994) Metastability in diffusing-reacting systems. *J. Cryst. Growth.* **142**, 225–235.

Prieto M., Fernández-González A., Putnis A., and Fernández-Díaz L. (1997) Nucleation, growth, and zoning phenomena in crystallizing $(Ba,Sr)CO_3$, $Ba(SO_4,CrO_4)$, $(Ba,Sr)SO_4$, and $(Cd,Ca)CO_3$ solid solutions from aqueous solutions. *Geochim. Cosmochim. Acta* **61**, 3383–3397.

Prieto M., Fernández-González A., and Martín-Díaz R. (2002) Sorption of chromate ions diffusing through barite-hydrogel composites: Implications for the fate and transport of chromium in the environment. *Geochim. Cosmochim. Acta* **66**, 783–795.

Reeder R. J. (1996) Interaction of divalent cobalt, zinc, cadmium, and barium with the calcite surface during layer growth. *Geochim. Cosmochim. Acta* **60**, 1543–1552.

Rock P. A., Casey W. H., McBeath M. K., and Walling E. M. (1994) A new method for determining Gibbs energies of formation of metal-carbonate solid solutions: 1. The $Ca_xCd_{1-x}CO_3$ (s) system at 298 K and 1 bar. *Geochim. Cosmochim. Acta* **58**, 4281–4291.

Sarig S. (1994) Fundamentals of aqueous solution growth. In *Handbook of Crystal Growth,*Vol. 2 (ed. D. T. J. Hurle), pp. 1217–1270. Elsevier.

Sposito G. (1986) Distinguishing adsorption from surface precipitation. In *Geochemical Processes of Mineral Surfaces* (eds. J. A. Davis and K. Hayes), pp. 217–228. Symposium Series 323. American Chemical Society.

Stipp S. L., Hochella M. F., Parks G. A., and Leckie J. O. (1992) Cd^{2+} uptake by calcite, solid-state diffusion, and the formation of solid-solution: Interface processes observed with near-surface sensitive techniques (XPS, LEED, and AES). *Geochim. Cosmochim. Acta* **56**, 1941–1954.

Tesoriero A. J. and Pankow J. F. (1996) Solid solution partitioning of Sr^{2+}, Ba^{2+}, and Cd^{2+} to calcite. *Geochim. Cosmochim. Acta* **60**, 1053–1063.

Wada N., Yamashita K., and Umegaki T. (1995) Effects of divalent cations upon nucleation, growth and transformation of calcium carbonate polymorphs under conditions of double diffusion. *J. Cryst. Growth* **148**, 297–304.

Walter L. M. and Morse J. W. (1985) The dissolution kinetics of shallow marine carbonates in seawater: A laboratory study. *Geochim. Cosmochim. Acta* **49**, 1503–1513.

Wen C. Y. (1968) Noncatalytic solid-fluid reaction models. *Ind. Eng. Chem.* **60,** *9*, 34–54.

Zachara J. M., Cowan C. E., and Resch C. T. (1991) Sorption of divalent metals on calcite. *Geochim. Cosmochim. Acta* **55**, 1549–1562.